

# Annealing temperature dependence of the electrically active profiles and surface roughness in multiple Al implanted 4H-SiC

F. Giannazzo<sup>1\*</sup>, F. Roccaforte<sup>1</sup>, D. Salinas<sup>2</sup>, V. Raineri<sup>1</sup>

<sup>1</sup>CNR-IMM, Stradale Primosole 50, 95121 Catania, Italy

<sup>2</sup>STMICROELECTRONICS, Stradale Primosole, 50, 95121 Catania, Italy

\* e-mail: giannazzo@imm.cnr.it

**Keywords:** Al implantation, electrical activation, scanning probe microscopy

**Abstract.** In the present work, we systematically studied the effect of the annealing temperature (from 1400 °C to 1650 °C) on the electrical activation of 4H-SiC implanted with multiple energy (from 40 to 550 keV) and medium dose ( $1 \times 10^{13} \text{ cm}^{-2}$ ) Al ions. The evolution of the acceptors ( $N_A$ ) and compensating donors ( $N_D$ ) depth profiles was monitored by the combined use of scanning capacitance microscopy (SCM) and scanning spreading resistance microscopy (SSRM). We demonstrated that the electrical activation of the implanted layer with increasing annealing temperature is the result of the increase in the acceptors concentration and of the decrease in the  $N_D/N_A$  ratio. Atomic force microscopy (AFM) morphological analyses indicated that the surface quality is preserved even after the 1650 °C annealing process.

## Introduction

Ion implantation is the most commonly applied method for selective area doping [1-4] of silicon carbide (SiC) and to locally modify the electrical properties of SiC based devices [5]. In particular, multiple Al and/or B ion implantation is used to obtain medium concentration ( $10^{17}$ – $10^{18} \text{ cm}^{-3}$ ), uniformly doped p-type wells in 4H-SiC, which are used as the active region for power devices applications [6]. High annealing temperatures are required to bring the implanted Al atoms to substitutional positions in the 4H-SiC lattice and to anneal the defects introduced by the implantation. Some of the defects, peculiarly related to the Al implant, exhibit a donor like behaviour, as indicated by some deep level transient spectroscopy studies, reporting a large density of centres located at  $E_D \sim 0.42 \text{ eV}$  below the conduction band edge in the 4H-SiC [7]. Those defects produce a strong compensation of the acceptors (substitutional Al atoms) present in the material and strongly affect the transport properties (free hole concentration and mobility), as indicated in several works [8]. In order to exhaustively characterize the electrical properties of the implanted sheet after annealing, it is necessary to determine the depth distribution of the acceptor centres and of the compensating centres in the Al implant profile. Furthermore, for most of the applications a very low surface roughness of the implanted 4H-SiC is a crucial requirement. Hence, an accurate morphological characterization is necessary to monitor the sample surface quality after annealing. In the present work, we systematically studied the effect of the annealing temperature on the evolution of the acceptors ( $N_A$ ) and donors ( $N_D$ ) depth profiles in a 4H-SiC layer implanted with multiple energy and medium dose ( $1 \times 10^{13} \text{ cm}^{-2}$ ) Al ions. According to TRIM numerical simulations [9], this Al dopant profile could produce a medium concentration ( $\sim 10^{18} \text{ cm}^{-3}$ ) uniformly doped p-type layer, if all Al atoms occupy substitutional positions. To characterize the samples, two different and complementary scanning probe microscopy based methods, i.e. scanning capacitance microscopy (SCM) and scanning spreading resistance microscopy (SSRM), were used in combination. The comparison between the resistivity ( $\rho$  vs depth) profile, obtained from SSRM, and the net doping profile ( $N = N_A - N_D$ ), obtained from SCM, allowed us to calculate the  $N_A$  and  $N_D$  profiles in the implanted layer.

## Experiment

For our experiments appropriate samples were chosen, i.e. n-type 4H-SiC substrates with a  $\sim 0.5$   $\mu\text{m}$  thick  $p^+$  doped ( $N_A-N_D=1\times 10^{18}$   $\text{cm}^{-3}$ ) buffer layer and a  $\sim 2$   $\mu\text{m}$  thick p-doped ( $N_A-N_D=1\times 10^{15}$   $\text{cm}^{-3}$ ) epitaxial layer on top. The  $p^+$  and  $p^-$  doped layers were used as reference levels for SCM and SSRM raw data calibration. Multiple ion implants were carried out at different energies (40, 160, 250, 350, 450 and 550 keV) on the samples heated at 400  $^\circ\text{C}$ . For each implant energy, an ion dose of  $1\times 10^{13}$   $\text{Al}^+/\text{cm}^2$  was used, in order to obtain  $\sim 700$  nm thick box-like Al profiles with  $\sim 1\times 10^{18}$   $\text{cm}^{-3}$  uniform concentration. The implanted samples were annealed in a Centrotherm furnace at different temperatures ranging from 1400  $^\circ\text{C}$  to 1650  $^\circ\text{C}$  for 30 minutes in Ar or Ar+SiH<sub>4</sub> ambient. In order to monitor the surface quality after different the thermal processes, the RMS roughness was measured both on the virgin, as-implanted and annealed samples by tapping mode atomic force microscopy (AFM) using a DI3100 equipment with Nanoscope V controller.

SCM [10,11] and SSRM [12] analyses were carried out on the angle bevelled surface of the implanted samples by connecting the AFM tip to the capacitance and current measuring equipments. In SCM analyses, the local value of the derivative of capacitance with respect to voltage ( $dC/dV$ ) was detected by the SCM sensor in response to the 0 Volt DC bias and 1 Volt modulating AC bias (100 kHz frequency) applied to the sample during the two dimensional scan by a conductive diamond coated AFM tip.

Local current measurements have been carried out by applying 2 Volt DC bias to the sample with respect to the conductive diamond coated AFM tip. A Keithley 428 current amplifier has been connected to the tip. The high pressures (GPa) exerted by the tip on the sample surface allows to break the native oxide and form an intimate metal-semiconductor contact with 4H-SiC.

## Results and discussion

In SCM analyses, the AC bias amplitude is high enough to completely ionise all the acceptor and donor (compensating) centres within the nanometric 4H-SiC volume underneath the tip, regardless of the depth of their energy levels within the bandgap. The amplitude of the SCM signal is related to the net dopant concentration ( $N=N_A-N_D$ ), while its sign to the doping type. The sign of the raw SCM profile in the Al implanted region is consistent with p-type doping after all annealing

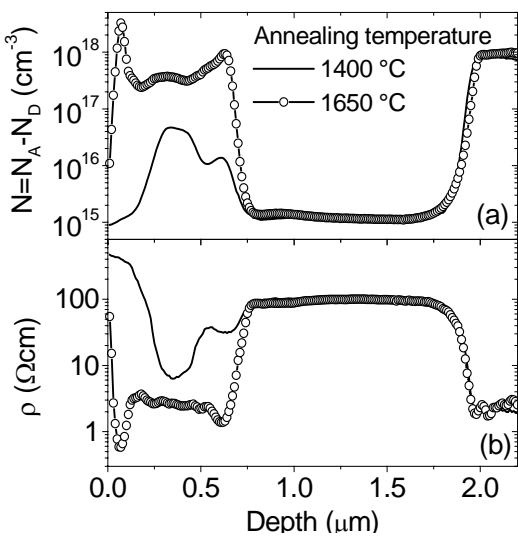


**Fig.1** Net doping concentration ( $N_A-N_D$ ) profile from SCM (a) and resistivity profile from SSRM (b) for the samples annealed at 1400  $^\circ\text{C}$  and 1650  $^\circ\text{C}$ .

temperatures, indicating that the acceptor concentration  $N_A$  is always higher than the compensating centers concentration  $N_D$  in the considered annealing conditions. Hence, the  $N=N_A-N_D$  versus depth profile has been extracted from SCM raw data profile, following the calibration method described in Ref. [11]. These profiles are reported in Fig.1(a) for the samples annealed at 1400  $^\circ\text{C}$  and 1650  $^\circ\text{C}$ .

In the current measurements carried out under the indicated operating conditions, the spreading resistance is the dominant contribution to the resistance encountered by the current flow from the tip to the sample back-contact. This contribution is directly related to the local resistivity  $\rho$  of the nanometric size 4H-SiC region underneath the tip. The  $\rho$  depth profiles extracted from the SSRM profiles on the samples annealed at 1400  $^\circ\text{C}$  and 1650  $^\circ\text{C}$  are reported in Fig.1(b).

After the annealing at 1400  $^\circ\text{C}$ , the net doping concentration  $N=N_A-N_D$  profile exhibits a peculiar shape with two peaks (at  $\sim 300$  nm and  $\sim 600$  nm depths), a very low concentration in the  $\sim 200$  nm surface region

and a valley at a depth of ~550 nm. The shape of resistivity profile qualitatively resembles the shape of the net doping profile. In particular very high resistivity values are obtained in the surface region, indicating a very strong compensation in that region. After annealing at 1650 °C, we obtained a

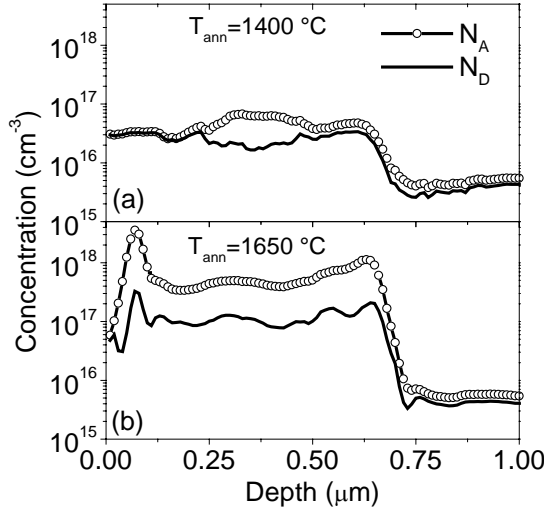


**Fig.2** Concentration vs depth profiles of acceptors  $N_A$  and compensating donors  $N_D$  for the samples annealed at 1400 °C (a) and 1650 °C (b).

significantly different net doping profile with a uniform concentration of  $\sim 4\div 5 \times 10^{17} \text{ cm}^{-3}$  extending over a depth of 600 nm and with a higher concentration ( $4 \times 10^{18} \text{ cm}^{-3}$ ) surface peak. Again, the resistivity profile shape resembles the net concentration profile shape.

The measured resistivity values are related to the local free carrier concentration  $p$  and to the mobility  $\mu_p$ , by the relation  $\rho = 1/(q \times p \times \mu_p)$ . Due to the energy of the acceptor levels for the two known substitutional Al configurations in the 4H-SiC lattice [13], at room temperature  $p$  is only a fraction of  $N_A$ . Moreover, its value is also affected by the local concentration of donor centres  $N_D$ , according to the neutrality equation:

$$p + N_D = \sum_{n=1}^2 \frac{N_{A,n}}{1 + \frac{p}{gN_V \exp\left(-\frac{E_{A,n} - E_V}{k_B T}\right)}} \quad (1),$$

where  $g$  is the degeneracy factor and  $N_V$  is the effective density of states in the valence band,  $k_B$  the Boltzmann constant and  $T$  the temperature (K). In the present work we assumed  $E_{A1} - E_V \sim 190 \text{ meV}$  and  $E_{A2} - E_V \sim 230 \text{ meV}$  [13].

The mobility  $\mu_p$  depends both on the donor and acceptor concentrations. This dependence can be described by the following semiempirical relation, which has been validated on a wide range of epitaxially doped p-type samples [14]:

$$\mu_p = \mu_p^{\min} + \frac{\mu_p^{\max} - \mu_p^{\min}}{1 + \left(\frac{N_A + N_D}{N_{ref}}\right)^\gamma} \quad (2),$$

where  $\mu_p^{\min} = 37.6 \text{ cm}^2 \text{ V}^{-1} \text{ s}^{-1}$ ,  $\mu_p^{\max} = 106.0 \text{ cm}^2 \text{ V}^{-1} \text{ s}^{-1}$ ,  $N_{ref} = 2.97 \times 10^{18} \text{ cm}^{-3}$  and  $\gamma = 0.356$  [14].

By jointly using the  $N$  and the  $\rho$  profiles in Fig.1(a) and (b), the profiles of the compensating centres  $N_D$  and acceptors  $N_A$  have been extracted. The results are reported in Fig.2(a) and (b) for the samples annealed at 1400 °C and 1650 °C, respectively.

The peculiar shape of the net doping profile after the annealing at 1400 °C (Fig.1(a) (line)) can be clearly explained in terms of the  $N_A$  and  $N_D$  profiles in Fig.2(a). In fact, the higher values of  $N_D$  are responsible both of the electrically inactive surface region and of the valley at ~550 nm depth in the  $N_A - N_D$  profile. After the annealing at 1650 °C, the  $N_D$  becomes a smaller fraction than  $N_A$ , except in the near surface region. Hence, the  $N = N_A - N_D$  depth profile is almost coincident with the  $N_A$  depth profile, with the only significant difference in the surface region. By calculating the area under the  $N_A$  and  $N_D$  profiles in the implanted region, the doses of the acceptors ( $D_A$ ) and donor centres ( $D_D$ ) were obtained. In Table.1 the percentage compensation ( $D_D/D_A$ ) and the percentage activation ( $D_A/D_{imp}$ ), where  $D_{imp} = 6 \times 10^{13} \text{ cm}^{-2}$  is the implanted Al dose, are reported as a function of the annealing temperature. It is worth noting the opposite behaviour of these two quantities. While the percentage compensation decreases from ~60% to ~18% with increasing the annealing temperature

	1400 °C	1500 °C	1650 °C
$D_A/D_{imp}$ (%)	4.9	16.3	74.8
$D_D/D_A$ (%)	60.4	31.6	17.9

**Table.1** Percent activation and percent compensation for the samples annealed at 1400 °C, at 1500 °C and 1650 °C

from 1400 °C to 1650 °C, the percentage activation, i.e. the fraction of Al atoms on substitutional sites, increases from ~5% to ~75%, for the same increase of annealing temperature.

In Fig.3, the comparison between the AFM morphological images in the samples annealed at 1400 °C (a) and at 1650 °C (b) is reported, together with the respective RMS roughness values. These analyses showed that RMS values lower than 0.3 nm are obtained even after annealing at 1650 °C.

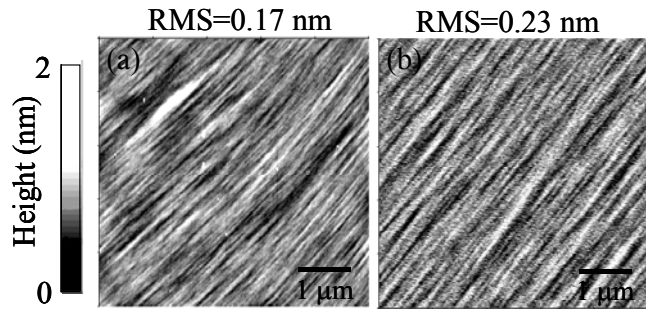


**Fig.3** AFM images of the samples annealed at 1400 °C and 1650 °C, respectively. The RMS roughness values are also reported on the figures.

## Conclusions

The acceptor and compensation profiles at room temperature in multiple Al ion implanted 4H-SiC were determined by jointly using SCM and SSRM. The evolution of those profiles has been followed after annealing at temperatures from 1400 °C to 1650°C, showing in details how the implanted layer electrical activation with increasing temperature is the result of a counter balance between the decrease in the percent compensation and an increase in the percent activation. AFM morphological analyses indicated that the surface quality is preserved even after the 1650 °C annealing process.

## Acknowledgement

The authors acknowledge A. Marino and S. Di Franco from CNR-IMM for their expertise assistance in Al ion implantation and sample preparation, respectively.

## References

- [1] Y. Negoro, T. Kimoto, H. Matsunami, F. Schmid and G. Pensl, *J. Appl. Phys.* Vol 96, (2004) p. 4916.
- [2] Y. Negoro, K. Katsumoto, T. Kimoto, and H. Matsunami, *J. Appl. Phys.* Vol 96, (2004) p. 224.
- [4] M. Canino, F. Giannazzo, F. Roccaforte, A. Poggi, S. Solmi, V. Raineri, and R. Nipoti, *Materials Science Forum* Vol. 556-557, (2007) p. 571.
- [5] F. Roccaforte, S. Libertino, F. Giannazzo, C. Bongiorno, F. La Via, and V. Raineri, *J. Appl. Phys.* Vol. 97, (2005) p. 123502.
- [6] N. S. Saks, A. K. Agarwal, S.-H. Ryu, and J. W. Palmour, *J. Appl. Phys.* Vol. 90, p. 2796 (2001).
- [7] S. Mitra, M. V. Rao, N. Papanicolaou, K. A. Jones, M. Derenge, O. W. Holland, R. D. Vispute, and S. R. Wilson, *J. Appl. Phys.* Vol. 95 (2004), p. 69.
- [8] N. S. Saks, A. V. Suvorov, and D. C. Capell, *Appl. Phys. Lett.* Vol. 84, (2004), p. 5195.
- [9] J. P. Biersack, *Nucl. Instrum. Methods Phys. Res. B* Vol. 35, (1988), p. 205.
- [10] F. Giannazzo, P. Musumeci, L. Calcagno, A. Makhtari and V. Raineri, *Mater. Sci. Semicond. Process.* Vol. 4, (2001), p. 195.
- [11] F. Giannazzo, L. Calcagno, V. Raineri, L. Ciampolini, M. Ciappa, E. Napolitani, *Appl. Phys. Lett.* Vol. 79, (2001), p. 1211.
- [12] J. Osterman, A. Hallén, and S. Anand, *Appl. Phys. Lett.* Vol. 81, (2002), p. 3004.
- [13] J. Pernot, S. Contreras, and J. Camassel, *J. Appl. Phys.* Vol. 98, (2005), p. 023706.
- [14] H. Matsuura, M. Komeda, S. Kagamihara, H. Iwata, R. Ishihara, T. Hatakeyama, T. Watanabe, K. Kojima, T. Shinohe, K. Arai, *J. Appl. Phys.* Vol. 96, (2004), p. 2708.